Journal of Organometallic Chemistry, 355 (1988) 385–400
Elsevier Sequoia S.A., Lausanne – Printed in The Netherlands

Reaction of $M_3\{\mu\text{-}H,\mu\text{-}O{=}CNMe_2\}(CO)_{10}$ (M = Ru or Os) with but-2-yne. Crystal and molecular structures of $M_3\{\eta^3\text{-}CH_2CHC(H)CH_3\}\{\mu\text{-}(CO),\mu\text{-}O{=}CNMe_2\}(CO)_8$ (M = Ru or Os) and $Ru_2\{\mu\text{-}O{=}CCMe{=}CMe(\eta^2\text{-}CMe{=}CHMe\}\text{-}\{\mu\text{-}O{=}CNMe_2)(CO)_5$ *

Neil M. Boag, Werner J. Sieber, Carsten E. Kampe, Carolyn B. Knobler and Herbert D. Kaesz *

Department of Chemistry and Biochemistry, University of California, Los Angeles, California, 90024-1569 (U.S.A.)

(Received April 29th, 1988)

Abstract

The complexes $M_3\{\mu\text{-}H,\mu\text{-}O{=}CR\}(CO)_{10}$ ($R = NMe_2$, M = Ru (**1a**) or Os (**1b**)) are observed to react with dimethylacetylene (**2**) under varying conditions. The reaction of **2** is observed with **1a** at 23°C requiring 12 h for completion in hexane. Three isolable products are obtained along with a trace of $Ru_3(CO)_{12}$: $Ru_3\{\eta^3\text{-}CH_2CHC(H)CH_3\}\{\mu\text{-}(CO),\mu\text{-}O{=}CNMe_2\}(CO)_8$ (**3a**, 35%), $Ru_2\{\sigma,\pi\text{-}\mu\text{-}C(Me){=}CHMe,\mu\text{-}O{=}CNMe_2\}(CO)_6$ (**4a**, 14%), and $Ru_2\{\mu\text{-}O{=}CCMe{=}CMe\text{-}(\eta_2\text{-}CMe{=}CHMe\}\{\mu\text{-}O{=}CNMe_2)(CO)_5$ (**5a**, 9%). For reaction of the tri-osmium complex **1b** with **2**, heating to 140°C is required using excess **2** as its own solvent under autoclave conditions; only the η^3-allyl derivative **3b** is obtained (28% conversion; 98% yield).

Structures of three of the new products have been determined using Picker (FACS-1) or Syntex $P\bar{1}$ four circle automated diffractometers and graphite-monochromatized Mo-K_α radiation. Complex **3a** crystallizes in the monoclinic space group $P2_1/n$; cell dimensions a 10.4734(13) Å, b 15.3589(19) Å, c 13.7645(17) Å, and β 99.041(3)°; calculated density 2.07 g cm^{-3}; 3831 unique reflections with $I > 3\sigma(I)$ were used in the refinement; final discrepancy indices, $R = 0.042$ and $R_w = 0.055$. This is one of three different crystallographic modifications with essentially the same molecular parameters.

Complex **3b** crystallizes in the monoclinic space group $P2_1/n$; cell dimensions a 15.3496(13) Å, b 28.9195(22) Å, c 9.7116(8) Å, and β 98.114(3)°; calculated density

* Dedicated to Professor Ernst Otto Fischer on the occasion of his 70th birthday, November 10, 1988.

0022-328X/88/$03.50

3.05 g cm^{-3}; 5897 unique reflections with $I > 3\sigma(I)$ were used in the refinement; final discrepancy indices, $R = 0.047$ and $R_w = 0.062$.

Complex **5a** crystallizes in the monoclinic space group $P\bar{1}$; cell dimensions a 7886(2) Å, b 10.987(3) Å, c 12.337(3) Å, α 96.88(2)°, β 87.18(2)°, and γ 104.36(2)°; calculated density 1.78 g cm^{-3}; 3872 unique reflections with $I > 3\sigma(I)$ were used in the refinement; final discrepancy indices, $R = 0.035$ and $R_w = 0.060$.

Metal atoms in all three structures were located by direct methods (MULTAN80). All other nonhydrogen atoms were then located by difference maps. Hydrogen atoms in the organic groups were included in structure factor calculations in calculated positions. Each of the crystals studied consists of discrete molecules of the complexes; crystals of **3a** and **3b** each consist of a triangle of metal atoms containing an η^3-methallyl fragment attached to one of the atoms along an edge also bridged by a CO group and a dimethylcarboxamido group. For **5a**, a dinuclear unit is observed which is bridged by a {μ-O=CCMe=CMe-(η^2-CMe=CHMe} group as well as a dimethylcarboxamido group. The metal–metal separations in the three structures are summarized as follows, Å, respectively: unbridged Ru–Ru (in **3a**) 2.867(1) and 2.829(1); bridged Ru–Ru separations 2.783(1) (in **3a**), and 2.681(1) (in **5a**). In **3b** the Os–Os separations for the two independent molecules of the unit cell are, respectively, Å: 2.848(1), 2.846(1) and 2.833(1), 2.871(1) (unbridged) and 2.814(1), 2.786(1) (bridged).

The position of the allyl group in products **3a** or **3b** as well as the point of attachment of the μ-O=CCMe=CMe-(η^2-CMe=C(H)Me group suggest that initial substitution of acetylene occurs on the metal to which the oxygen of the μ-O=$CNMe_2$ group is attached. This follows the path of PR_3 or ^{13}CO substitution observed for these and related edge double-bridged derivatives.

Introduction

Earlier, we showed that the edge double-bridged complexes Ru_3\{μ-H,μ-O=CR\}$(CO)_{10}$ (R = Et, Me, Ph, or NMe_2) react with ethylene under mild conditions to give *gem*-dinuclear bis-acyl derivatives [1]. For the analogous osmium complexes, tri-nuclear bis acyl derivatives are obtained in equilibrium mixture of (85%/15%) *vic-*/ and *gem*-Os_3\{μ-O=C(R)\}$_2(CO)_{10}$ [2].

In the present work we extend our studies of the chemistry of the edge double-bridged complexes M_3\{μ-H,μ-O=$CNMe_2$\}$(CO)_{10}$ (M = Ru (**1a**) [3] or Os (**1b**) [4]) to their reaction with but-2-yne; preliminary communications of this work have appeared [5]. We have also studied the reactions with aryl acetylenes, to be communicated separately [6].

Results of the syntheses

The transformations observed in this study are summarized in Scheme 1.

The products shown in the Scheme are those which could be isolated by chromatography; **3a** and **4a** are easily separated on silica gel, however, **5a** can only be eluted from grade 4 alumina as support. Of the products shown in Scheme 1, **3a** and **3b** are the most stable to handling. We observe a general instability under chromatography for the other products. Re-chromatography of **4a**, for example,

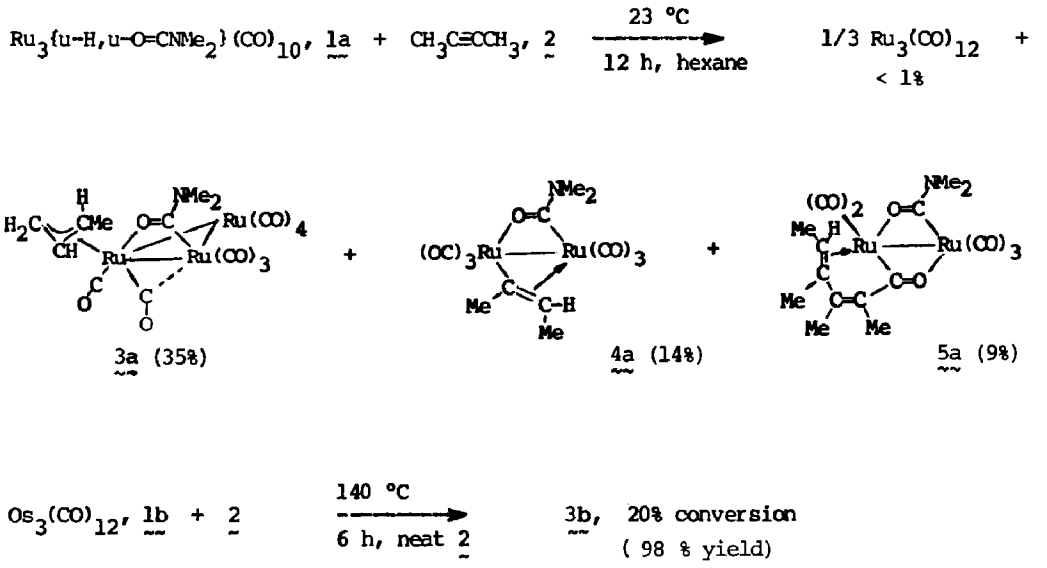

Scheme 1

always gives smaller recovered yields. Finally, some minor constituents of the reaction mixture could not be removed from either of the two column supports used in this study, representing no doubt, the ruthenium content of the starting material unaccounted for in the products.

Reaction of the osmium analogue **1b** required elevation of temperature. At 140 °C only 20% of **1b** is converted to product which is exclusively the η^3-methallyl complex **3b**.

Carbonyl absorptions in the IR and ^{1}H NMR data are given in Table 1. We assign the σ,π-vinyl structure to complex **4a** by similarity of the carbonyl absorptions to those of similar derivatives characterized by X-ray structure determinations [6]. The data on the other derivatives was found to be insufficient to determine molecular structures; two of the ruthenium containing derivatives and the triosmium complex **3b** were subject to structure determination. The latter was examined because its spectroscopic data did not indicate a bridging CO as seen for the triruthenium analog **3a**. Indeed it turned to be structurally homologous to **3a**. The structure determinations are described in the second part of the Experimental Section and results are discussed in the section which follows.

Experimental

General. Solvents and reagents were of commercial reagent grade and were dried and redistilled under nitrogen. The petroleum ether cited throughout this work is that from Mallinckrodt ("AR", b.pt. 36–60 °C). But-2-yne (**2**) was obtained from Farchan Laboraties Inc. (new address: 4702 E. 355 St., Willoughby, OH 44094). The starting metal complexes **1a** and **1b** were prepared according to literature procedures [3] and [4], respectively.

Because some of the products in this work are not air stable, all manipulations including chromatographic separations were routinely carried out under a purified

Table 1

Spectroscopic data

ν(CO) (cm^{-1}) [a]	
3a	2088m 2043vs 2018m 2009s 1997m 1993m 1973w 1889w
3b	2094m 2045vs 2018s 2005s 1991m 1977vw 1967w 1897vw
4a	2078m 2045vs 2005s 1996m 1980m 1980m 1977m
5a	2067vs 2010vs 2000vs 1971s 1950m
^{1}H NMR/ppm (J(Hz)) [b]	
3a	2.03 (d, J = 6.1 Hz, CH_3); 3.49 (dxq, J 12.2, 6.1 Hz, H(1)); 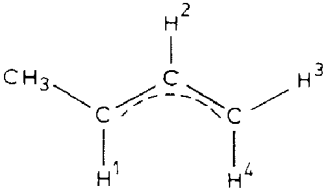 5.01 (dxdxd, J 12.2,12.2,7.2 Hz, H(2)), 4.43 (d, J 7.2 Hz, H(3)); 1.62 (d, J 12.2 Hz, H(4))
μ-O=CN(Me)$_2$: 3.17 (s) 2.69 (s).	
5a	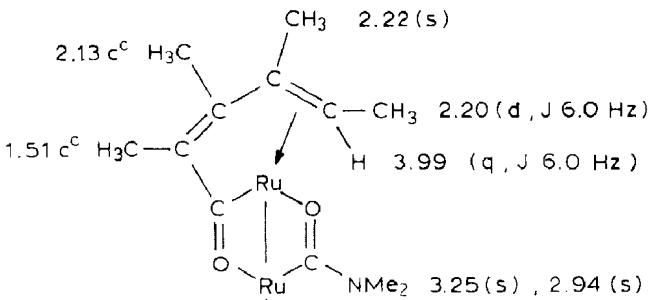

[a] Hexane solution; m, medium; s, strong; w, weak, vs, very strong. [b] 90 MHz, 26° C, $C_6D_5CD_3$ sol'n; s, singlet; d, doublet; q, quartet. [c] c, complex multiplet, $v_{1/2}$ ca. 1 Hz.

nitrogen atmosphere using Schlenk techniques. Carbonyl infrared spectra were recorded on a Nicolet MX-1 FT-IR spectrometer. ^{1}H and ^{13}C NMR spectra were recorded on a JEOL FX90Q spectrometer; ^{1}H NMR were calibrated against internal residual $CHCl_3$ at $\delta = 7.25$ or tetramethylsilane (TMS).

Reaction of but-2-yne (2) with $Ru_3\{\mu\text{-}H,\mu\text{-}O{=}CNMe_2\}(CO)_{10}$ (1a). To a quantity of **1a** (0.65 g, 1 mmol) in 50 ml hexane, is added 1 ml **2** (ca. 20 mmol) and the mixture stirred under N_2 at 23 °C for 12 h. Solvent and excess **2** are removed under vacuum and the beige powdery residue extracted twice with 50 ml aliquots of hexane. The solvent volume is reduced to 15 ml and placed on an alumina column (Merck, 70-230 mesh, grade IV; 2 cm dia. × 25 cm length). Following a pale yellow band of a trace of $Ru_3(CO)_{12}$ (ca. < 1%), two fractions are eluted; starting with hexane, an orange-yellow band is eluted to give an oil proving to be a mixture of starting material, **1a**, and the products **3a** and **4a**. These are separated on a silica-gel column (see below). Continuing elution of the alumina column with a mixture of hexane/CH_2Cl_2 (4:1), a second band is obtained which contains **5a**. This is isolated as a yellow oil and recrystallized from hexane. Yield: 49 mg (9% based on **1a**). Spectroscopic data are given in Table 1; structure determination is described below.

Separation of the above-mentioned mixture of **1a, 3a** and **4a** is achieved on a silica gel column (Baker Analyzed, 60-200 mesh; 2 cm dia. × 20 cm length). Eluting first with hexane, an orange band is separated to give an orange oil which proves to be **3a**. This may be recrystallized from pentane. Yield: 0.24 g (35% based on **1a**). This compound was also characterized by X-ray structure determination (see below); spectroscopic data are given in Table 1, above.

A second (yellow) band, separating away from the first band, is next eluted with ca. 100 ml hexane; this band proves to be recovered starting material (ca. 11.4 mg). Using a mixture of hexane/CH_2Cl_2 (4:1) a third band (yellow) is next eluted. This fraction yields a yellow oil which is assigned as product **4a** through spectroscopic means. Yield: 69 mg (14% based on **1a**).

Reaction of 2 with $Os_3\{\mu\text{-}H,\mu\text{-}O{=}CNMe_2\}(CO)_{10}$ (1b). A quantity of **1b** (170 mg, 0.18 mmol) is placed in a 10 ml autoclave to which is also added 2 ml of **2**. The autoclave is closed under an atmosphere of N_2 and heated to 140 °C for 6 h. After cooling to room temperature, the autoclave is opened and the dark yellow solution is transferred to a Schlenk tube. Excess **2** is removed under an oil-pump vacuum and the yellow-brown residue is suspended in 10 ml hexane and transferred to a silica gel column (same as above, 30 cm length). Two fractions are eluted; starting with hexane, a yellow band is obtained giving rise to an oil. Recrystallization from hexane followed by structure determination (see below) established this product as **3b**. Yield before recrystallization: 35 mg (20% based on **1b**). Continuing the elution with hexane, a second very broad yellow band is obtained which proved to be unreacted starting material, **1b**, 110 mg. A dark brown material which could not be removed by CH_2Cl_2 or acetone, remains at the top of the column.

Crystallographic study

Data collection

Air and X-ray stable single crystals were obtained for each of the three compounds whose structures were determined. Data for each of the crystals and

Table 2

Crystal data for $M_3\{\eta^3\text{-}CH_2CHC(H)CH_3\}\{\mu\text{-}(CO),\mu\text{-}O{=}CNMe_2\}(CO)_8$ (M = Ru, **3a**, M = Os, **3b**) and $Ru_2\{\mu\text{-}O{=}CCMe{=}CMe(\eta^2\text{-}CMe{=}CHMe)\}\{\mu\text{-}O{=}CNMe_2\}(CO)_5$ (**5a**)

	3a	**3b**	**5a**
Formula	$C_{16}H_{13}NO_{10}Ru_3$	$C_{16}H_{13}NO_{10}Os_3$	$C_{17}H_{19}NO_7Ru_2$
Formula wt.	682.49	949.88	551.48
a (Å)	10.4734(13)	15.3496(13)	7.886(2)
b (Å)	15.3689(19)	28.9195(22)	10.987(3)
c (Å)	13.7645(17)	9.7116(8)	12.337(3)
α (°)			96.88(2)
β (°)	99.041(3)	98.114(3)	87.18(2)
γ (°)			104.36(2)
V (Å^3)	2186.35	4276.62	1027.8(5)
Z	4	8	2
ρ(calc) (g cm^{-3})	2.07	3.05	1.78
Crystal system	Monoclinic [a]	Monoclinic [a]	Triclinic [a']
Space group	$P2_1/n$	$P2_1/n$	$P\bar{1}$
Crystal size (approx.) (mm)	$0.13\times0.14\times0.27$	$0.19\times0.22\times0.46$	$0.25\times0.25\times0.40$
Boundary faces	$\bar{1}11$ $11\bar{1}$ $1\bar{1}\bar{1}$ $\bar{1}\bar{1}0$ $\bar{1}\bar{1}1$ $\bar{1}0\bar{1}$ 101 [b]	$1\bar{1}0$ $\bar{1}\bar{1}0$ $\bar{1}10$ 110 $11\bar{1}$ $\bar{1}2\bar{1}$ 001 [c]	$0\bar{1}\bar{2}$ 010 001 $0\bar{1}0$ $\bar{1}0\bar{1}$ 100 [d]
Temperature (K)	298	298	298
Abs. coeff. (μ) (cm^{-1}) [e]	20.551	178.986	14.758
Transmission factors (F^2)	0.7186–0.8300	0.0241–0.1130	0.6860–0.7757
θ–2θ Scan rate (deg min^{-1})	6.0	6.0	12.0
Scan width [f]	−1.3 to +1.4	−1.3 to +1.4	−1.4 to +1.4
2θ limits (deg)	0–50	0–50	0–55
Unique reflections	4233	8478	4759
Unique data ($I_0 > 3I_0$) [g]	3831	5897	3872
Total no. of variables [h]	475	541	508
R [i]	0.042	0.047	0.035
R_w [j]	0.055	0.062	0.060
GOF [k]	1.7238	2.080	2.058

[a] Observations $+h$, $+k$, $\pm l$; [a'] Observations h, $\pm k$, $\pm l$. [b,c,d] At distances from a common point, respectively (mm): (b) 0.0 0.0 0.135 0.054 0.135 0.0 0.27; (c) 0.189 0.0 0.0 0.216 0.0 0.0 0.459; (d) 0.25 0.0 0.0 0.25 0.0 0.40. [e] Radiation: Mo-K_α 0.7107 Å. [f] deg below Mo-K_α to deg above Mo-K_α. [g] Used in refinement. [h] In the last refinement. [i] $R = \Sigma(||F_0| - |F_c||)/\Sigma|F_0|$. [j] $R_w = [\Sigma w(|F_0| - |F_c|)^2/\Sigma w|F_0|^2]^{1/2}$; $w = 1/(\sigma^2|F_0|)$. [k] Error in observation of unit wt. = $[\Sigma w(|F_0| - |F_c|)^2/(N_0 - N_v)]^{1/2}$.

parameters related to data collection and refinement are given in Table 2. All crystals were grown by gradual cooling; a Schlenk tube containing a solution of the complex under N_2 is placed in a small, empty Dewar flask which in turn is placed in the freezer compartment of a refrigerator and allowed slowly to equilibrate with its temperature of $-30\,^{\circ}C$. For **3a**, orange or dark orange crystals are obtained from pentane solution. In fact, three different crystalline modifications were obtained which led to three independent structure determinations. Since these differed only in the packing of the molecules but not, within experimental error, in the molecular parameters, only one of these is described here.

For **3b** or **5a**, dark yellow or yellow crystals (respectively) are obtained from hexane solutions. The crystals were each glued to the tip of a glass fiber and mounted on a goniometer head of a Syntex $P\bar{1}$ (**5a**) or Picker (FACS-1) four-circle automated diffractometer (**3a** and **3b**); The latter was modified at U.C.L.A. by C.E. Strouse for operation under control of a VAX 11/750 computer.

Lattice parameters and standard errors were determined by least squares refinement of the angular settings of a number of reflections (Mo-K_α) centered on the diffractometer: for **3a**, 27 peaks in the range $11° < 2\theta < 21°$; for **3b**, 26 peaks in the range $11° < 2\theta < 21°$; for **5a**, 19 peaks in the range $10° < 2\theta < 21°$. The refined unit cell parameters and other specifics relevant to the data collection are given in Table 2. For **3b**, there are two independent molecules in the unit cell (cf. Table 2); these are designated as **3b** and **3b'** when molecular parameters are cited.

Background for each peak was determined from the peak profile. The intensities of three standard reflections were recorded after every 97 intensity measurements to monitor crystal and diffractometer stability; standard reflections, respectively, for **3a**, $(0,3,\bar{4})$, $(3,2,\bar{2})$, (1,5,0); for **3b**, $(8,28,\bar{4})$, $(0,0,\overline{15})$, (23,30,15); for **5a**, $(1,0,\bar{2})$, (1,0,3) and $(0,\bar{5},5)$. The variations in the standards were random for all three samples, all showing deviations from the respective means values of less than 2%.

A survey of the complete data set for each structure showed systematic absences consistent with assignment of the space group shown in Table 2: for **3a** and **3b**, reflections $(h,0,l)$ $h + l \neq 2n$, and $(0,k,0)$ $k \neq 2n$; no absences were observed for **5a**. The total number of independent reflections measured for each compound and range of 2θ are given in Table 2, as well as the number of reflections used in the solution and refinement of each structure. All of the latter reflections were corrected for Lorentz and polarization effects and converted to $|F_0|$ and $\sigma(|F_0|)$ by means of the CARESS program (see next paragraph for description of computer programs).

Solution and refinement of the structures

All calculations were performed on a VAX 11/750 computer (Chemistry Department of UCLA). Programs used for the structure determination consist in all cases of local modification edited by Dr. C.E. Strouse and his research group: for data reduction, CARESS, originally written by R.W. Broach (Univ. of Wisconsin) and P. Coppens, P. Becker and R.H. Blessing (SUNY, Buffalo NY); for Patterson and for Fourier analyses, and for adaptations of MULTAN80, P. Main (Univ. of York, UK); for full matrix least-squares and error analysis, ORFLS and ORFFE, W.R. Busing, K.O. Martin and H.A. Levy (Oak Ridge National Lab., TN); for absorption correction, ABSN, P. Coppens; for least-square planes, MG84, P. Gantzel and K.N. Trueblood; for thermal ellipsoid plot program, ORTEP II, C.K. Johnson (Oak Ridge Nat. Lab.); for structure factor table listing, PUBLIST, E. Hoel.

(*Continued on p. 394*)

Table 3

Positional parameters

Atom	x	y	z
Part a. $Ru_3\{\eta^3\text{-}CH_2CHC(H)CH_3\}\{\mu\text{-}(CO),\mu\text{-}O{=}CNMe_2\}(CO)_8$ **(3a)**			
C(11)	−0.01092(91)	−0.00839(59)	−0.18339(65)
C(12)	−0.15763(95)	−0.14339(71)	−0.41142(70)
C(13)	−0.26071(102)	−0.05135(66)	−0.27142(68)
C(14)	−0.06469(89)	0.02660(71)	−0.38064(65)
C(21)	−0.20091(93)	−0.26443(67)	−0.25396(68)
C(22)	0.04654(91)	−0.30834(62)	−0.21245(67)
C(31)	0.18449(86)	−0.08188(60)	−0.34163(64)
C(32)	0.29094(110)	−0.24581(70)	−0.26168(79)
C(33)	0.07481(88)	−0.24169(65)	−0.40602(73)
C(71)	0.18017(74)	−0.13628(48)	−0.13891(55)
C(72)	0.29429(96)	−0.06933(59)	−0.01082(69)
C(73)	0.38958(106)	−0.06680(67)	−0.14185(76)
C(74)	−0.18470(84)	−0.16697(57)	−0.06853(62)
C(75)	−0.16734(90)	−0.25579(59)	−0.04949(66)
C(76)	−0.05388(97)	−0.29567(62)	−0.02337(70)
C(77)	−0.03105(116)	−0.39324(81)	−0.01384(88)
N(71)	0.28330(62)	−0.09316(45)	−0.09351(48)
O(11)	0.02560(77)	0.03370(46)	−0.11826(49)
O(12)	−0.20355(79)	−0.18069(54)	−0.48003(55)
O(13)	−0.35941(77)	−0.03584(62)	−0.25416(60)
O(14)	−0.05053(83)	0.08717(51)	−0.42490(53)
O(21)	−0.28904(77)	−0.29611(57)	−0.30243(55)
O(22)	0.07711(77)	−0.37975(45)	−0.21897(58)
O(31)	0.22563(68)	−0.02490(49)	−0.37924(50)
O(32)	0.38399(85)	−0.28524(63)	−0.25260(76)
O(33)	0.04312(81)	−0.28107(54)	−0.47661(56)
O(71)	0.09444(49)	−0.15428(33)	−0.08462(36)
Ru(1)	−0.09045(6)	−0.07224(5)	−0.30034(5)
Ru(2)	−0.06317(6)	−0.21760(4)	−0.17267(5)
Ru(3)	0.13249(6)	−0.18270(5)	−0.28253(5)
Part b. $Os_3\{\eta^3\text{-}CH_2CHC(H)CH_3\}\{\mu\text{-}(CO),\mu\text{-}O{=}CNMe_2\}(CO)_8$ **(3b)**			
C(11)	0.67327(128)	0.27028(73)	0.76572(209)
C(12)	0.52939(116)	0.37322(66)	0.61356(202)
C(13)	0.70664(166)	0.36026(74)	0.68061(240)
C(14)	0.58919(169)	0.34175(66)	0.87496(240)
C(21)	0.57811(144)	0.33162(59)	0.35240(207)
C(22)	0.48209(130)	0.25497(68)	0.34695(202)
C(31)	0.44492(131)	0.26930(67)	0.79510(199)
C(32)	0.37132(116)	0.22006(59)	0.55066(200)
C(33)	0.38201(115)	0.31428(60)	0.55159(200)
C(71)	0.54866(107)	0.20019(54)	0.62910(159)
C(72)	0.61901(150)	0.13335(66)	0.70283(245)
C(73)	0.48972(137)	0.15884(66)	0.00026(208)
C(74)	0.74133(140)	0.27490(84)	0.47419(238)
C(75)	0.71061(148)	0.26818(60)	0.32494(229)
C(76)	0.65838(148)	0.23198(57)	0.28174(188)
C(77)	0.62191(188)	0.22524(70)	0.13012(228)
N(71)	0.55131(106)	0.16926(47)	0.70621(156)
O(11)	0.71541(93)	0.24022(45)	0.81457(146)
O(12)	0.49110(110)	0.40248(48)	0.55943(161)
O(13)	0.76845(124)	0.38113(70)	0.67000(236)
O(14)	0.58554(149)	0.35388(56)	0.99156(172)

Table 3 (continued).

Atom	x	y	z
Part b. $Os_3\{\eta^3\text{-}CH_2CHC(H)CH_3\}\{\mu\text{-}(CO),\mu\text{-}O{=}CNMe_2\}(CO)_8$ **(3b)**			
O(21)	0.56771(113)	0.36784(48)	0.30545(141)
O(22)	0.42751(103)	0.24381(60)	0.26138(157)
O(31)	0.43274(113)	0.27280(50)	0.90931(147)
O(32)	0.31527(100)	0.19447(50)	0.52001(163)
O(33)	0.32916(102)	0.34058(52)	0.50716(168)
O(71)	0.60797(80)	0.21102(39)	0.55106(109)
Os(1)	0.60547(5)	0.32332(2)	0.69745(7)
Os(2)	0.59429(5)	0.27515(2)	0.32978(1)
Os(3)	0.46073(4)	0.26390(2)	0.60797(1)
C(41)	0.87178(114)	0.05013(55)	0.31233(176)
C(42)	0.75537(124)	−0.06787(73)	0.25214(194)
C(43)	0.83414(154)	−0.00806(76)	0.09458(242)
C(44)	0.92613(136)	−0.03861(55)	0.36496(187)
C(51)	0.60129(141)	−0.00769(73)	0.17427(225)
C(52)	0.58557(126)	0.03833(64)	0.41387(225)
C(61)	0.83823(150)	−0.02378(58)	0.61981(179)
C(62)	0.67297(140)	0.01096(53)	0.68158(206)
C(63)	0.67550(128)	−0.05817(55)	0.49737(172)
C(81)	0.76714(116)	0.07031(51)	0.51815(174)
C(82)	0.85134(138)	0.08115(68)	0.74977(179)
C(83)	0.83516(141)	0.14564(63)	0.58168(217)
C(84)	0.70178(136)	0.07955(68)	0.09485(207)
C(85)	0.61040(157)	0.08719(60)	0.09088(225)
C(86)	0.57613(131)	0.10484(70)	0.20413(243)
C(87)	0.48108(199)	0.11038(105)	0.21184(359)
N(81)	0.81516(100)	0.09764(43)	0.61264(154)
O(41)	0.90509(94)	0.08575(47)	0.32122(143)
O(42)	0.72672(110)	−0.10420(48)	0.22756(187)
O(43)	0.84264(170)	−0.00808(72)	−0.01925(181)
O(44)	0.99123(94)	−0.05444(46)	0.41221(154)
O(51)	0.56382(132)	−0.03685(57)	0.11566(193)
O(52)	0.52559(98)	0.04386(52)	0.47074(185)
O(61)	0.90027(108)	−0.03885(48)	0.67923(158)
O(62)	0.64059(107)	0.01480(54)	0.78341(152)
O(63)	0.64009(11)	−0.09425(47)	0.48363(153)
O(81)	0.73297(70)	0.09171(34)	0.40545(105)
Os(4)	0.81830(4)	−0.00989(2)	0.28550(7)
Os(5)	0.66004(4)	0.04126(2)	0.27398(7)
Os(6)	0.73005(4)	0.00049(2)	0.52536(7)
Part c. $Ru_2\{\mu\text{-}O{=}C{-}CMe{=}CMe\text{-}(\eta^2\text{-}CMe{=}CHMe\}\{\mu\text{-}O{=}CNMe_2\}(CO)_5$ **(5a)**			
C(11)	0.54754(72)	0.46810(59)	0.15804(50)
C(12)	0.56844(78)	0.38576(56)	0.36099(50)
C(13)	0.53670(76)	0.63947(54)	0.35562(50)
C(21)	0.22548(79)	0.23374(56)	0.06882(49)
C(22)	0.30190(79)	0.14834(55)	0.25550(50)
C(31)	0.21828(64)	0.51666(45)	0.21046(39)
C(32)	0.35131(87)	0.73251(55)	0.16949(57)
C(33)	0.04337(87)	0.63166(59)	0.12685(54)
C(41)	0.14236(64)	0.32493(43)	0.38659(37)
C(42)	0.00484(68)	0.25589(48)	0.45525(40)
C(421)	−0.02790(83)	0.31299(59)	0.56888(44)
C(43)	−0.09541(71)	0.14655(49)	0.40525(43)
C(431)	−0.24414(94)	0.06130(63)	0.46032(54)

Table 3 (continued)

Atom	x	y	z
Part c. $Ru_2\{\mu\text{-}O{=}C{-}CME{=}CMe\text{-}(\eta^2\text{-}CMe{=}CHMe\}\{\mu\text{-}O{=}CNMe_2\}(CO)_5$ ***(5a)***			
C(44)	−0.06968(73)	0.10551(47)	0.28548(45)
C(441)	−0.05694(98)	−0.03215(54)	0.25870(56)
C(45)	−0.12175(70)	0.16825(50)	0.20914(46)
C(451)	−0.18641(94)	0.11129(73)	0.09745(54)
N(31)	0.20626(60)	0.62288(40)	0.17233(35)
O(11)	0.62405(63)	0.46190(56)	0.07697(40)
O(12)	0.65156(70)	0.33388(52)	0.39970(42)
O(13)	0.61105(71)	0.73693(44)	0.39414(46)
O(21)	0.26016(73)	0.22194(52)	−0.02139(36)
O(22)	0.37961(71)	0.07751(48)	0.27310(49)
O(31)	0.08281(46)	0.42372(32)	0.20123(30)
O(41)	0.23379(45)	0.43108(31)	0.42154(27)
Ru(01)	0.42106(5)	0.47190(4)	0.28964(3)
Ru(02)	0.17507(5)	0.26197(3)	0.22652(3)

Scattering factors for neutral osmium, ruthenium, nitrogen, oxygen and carbon atoms were taken from Table 2.2A or ref. [7a] while those for hydrogen were from Stewart et al. [7b]. Both real (f') and imaginary (f'') components of anomalous dispersion were included for osmium and ruthenium using the values in Table 2.3.1. of ref. [7a]. The function minimized during least-squares refinement and the discrepancy indices are given in Table 2 *.

Reasonable positions for all the metal atoms in each of the three structures were obtained either by Patterson method (for **5a**) or by direct methods (MULTAN80, for **3a** and **3b**). Full-matrix least-squares refinement on the metal atoms with isotropic temperature factors followed by difference Fourier syntheses in each case revealed the positions of other atoms and, after further refinement, the positions of all non-hydrogen atoms. The data were also corrected for the effect of absorption, see Table 2. Least-squares refinement first with anisotropic thermal parameters for all the metal atoms and then, with anisotropic thermal parameters for all non-hydrogen atoms, afforded the R factors shown in Table 2.

At this stage, for **3a** and **5a**, it was possible to locate all hydrogen atoms on difference electron density maps. For **3b**, we were able to locate all the hydrogen atoms on only one of the crystallographically independent molecules in the unit cell, but only two of the hydrogen atoms in the second molecule, H(731), H(751). The positions of the located hydrogen atoms were not refined but used only for calculation of the final structure factors given in Table 2. Atomic positional parameters are given in Table 3, Part a, b, and c.

* The observed and calculated structure factor amplitudes as well as Tables of derived atomic positions (for hydrogen), thermal parameters and complete listings of interatomic distances and angles have been deposited with the National Auxiliary Publications Service, document No. 04627 FOR 44 pages of supplementary material. Order from NAPS c/o Microfiche Publications, P.O. Box 3513, Grand Central Station, New York, N.Y. 10163-3513. Remit in advance, in U.S. Funds only, $14.75 for photocopies or $4.00 for microfiche. Outside the U.S. and Canada, add postage of $4.50 for the first 20 pages and $1.00 for each of 10 pages of material thereafter, or $1.50 for microfice postage.

Description of the structures and discussion

Overall structures. The crystal of the three derivatives each consist of discrete molecular units; that of **3b** consists of two independent molecules in the unit cell, A and B. The geometry and atom numbering for **3a** is given in Fig. 1, while that for molecule B of **3b** is given in Fig. 2; the numbering of molecule A of **3b** is identical to that shown for **3a** in Fig. 1. The geometry and atomic numbering for **5a** is shown in Fig. 3. Selected interatomic distances and angles for the three derivatives are given in Tables 4 and 5.

Cluster nuclearity and metal–metal bonding. It is noteworthy that the trinuclear unit has remained intact in formation of the complexes **3a** and **3b**, while dinuclear complexes are observed for **4a** and **5a**. The formation of a second acyl group in **5a** bridging the same two metals connected to the (μ-O=CNMe$_2$) group is no doubt responsible for cluster degradation. This parallels the formation of the di-nuclear bis-acyl derivatives Ru$_2$\{μ-O=C(Et),μ-O=CR\}(CO)$_6$ (R = Et, Me, Ph, or NMe$_2$) obtained in the reaction of ethylene with the trinuclear edge double-bridged complexes Ru$_3$\{μ-H,μ-O=CR\}(CO)$_{10}$ [1]. Were the tri-nuclear assembly to have remained intact, the bond order between the doubly bridged metal atoms would be 0, owing to the presence of two three-electron donating groups along the metal–metal bond. Instead, an Ru(CO)$_4$ group is split off, while retaining the bond between the doubly-bridged Ru atoms. Indeed this bond, Ru(1)–Ru(2) 2.681(1) Å in **5**, is significantly shortened compared to the other singly-bonded Ru–Ru separations observed here and elsewhere [1,8]. The other metal–metal separations (Tables 4 and 5) are all in the range expected for single Ru–Ru or Os–Os bonds.

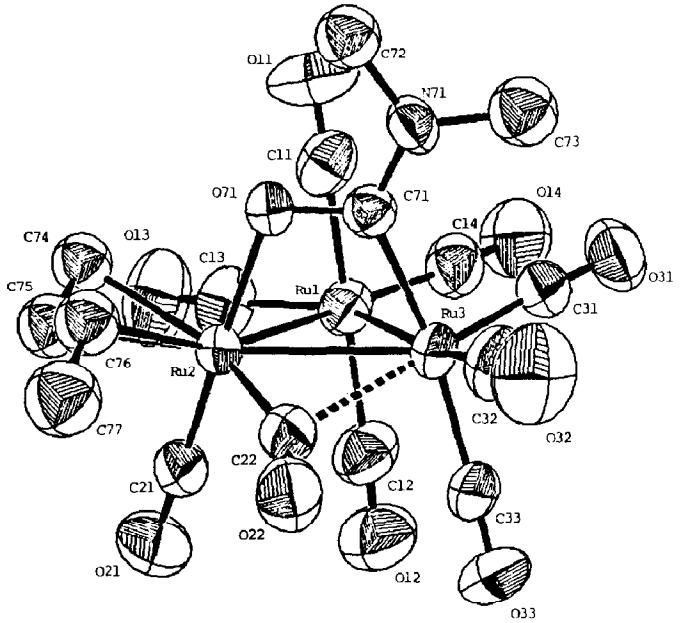

Fig. 1. ORTEP projection for **3a**, Ru$_3$\{η^3-CH$_2$CHC(H)CH$_3$\}\{μ-(CO),μ-O=CNMe$_2$\}(CO)$_8$; thermal ellipsoids at 50% probability. Hydrogen atoms are omitted (from the η^3-CH$_2$CHC(H)CH$_3$ group) for clarity.

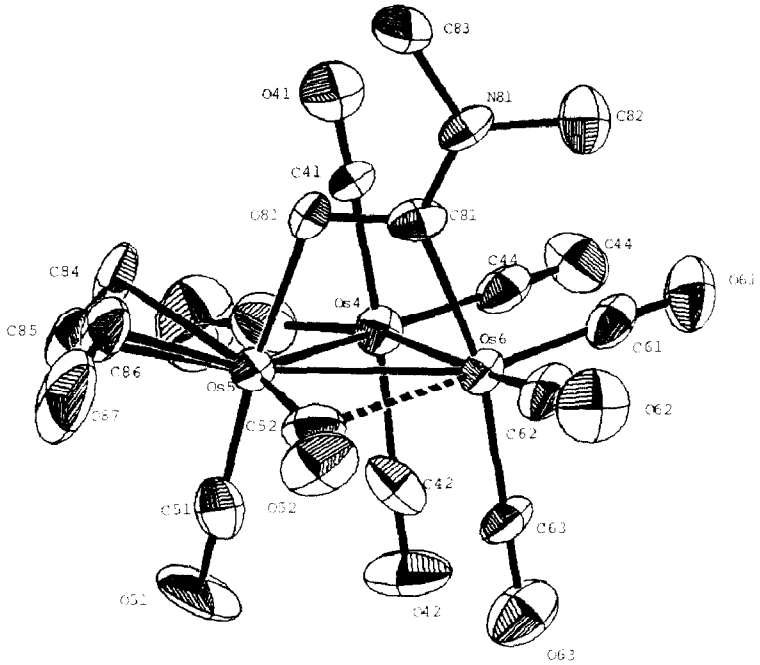

Fig. 2. ORTEP projection for molecule B of **3b**, $Os_3\{\eta^3\text{-}CH_2CHC(H)CH_3\}\{\mu\text{-}(CO),\mu\text{-}O{=}CNMe_2\}(CO)_8$; thermal ellipsoids at 50% probability. Hydrogen atoms are omitted (from the $\eta^3\text{-}CH_2CHC(H)CH_3$ group) for clarity. The labelling of molecule A is identical as shown for **3a** in Fig. 1.

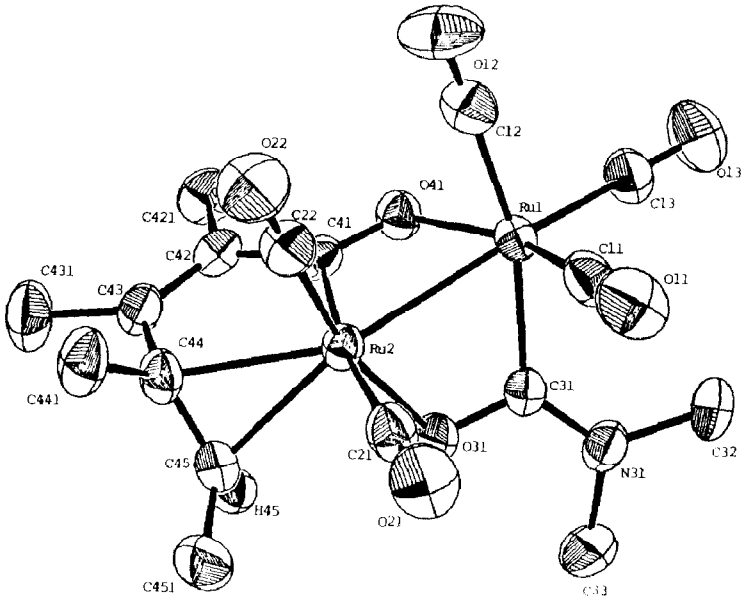

Fig. 3. ORTEP projection for **5a**, $Ru_2\{\mu\text{-}O{=}CCMe{=}CMe\text{-}(\eta^2\text{-}CMe{=}CHMe\}\{\mu\text{-}O{=}CNMe_2\}(CO)_5$; thermal ellipsoids at 50% probability. Hydrogen atoms are omitted for clarity.

Table 4

Selected interatomic separations and angles for $M_3\{\eta^3\text{-}CH_2CHC(H)CH_3\}\{\mu\text{-}(CO),\mu\text{-}O{=}CNMe_2\}(CO)_8$ [a]

M–M (Å)					
3a, Ru–Ru		**3b**(A) Os–Os		**3b**(B)	
(1)–(2)	2.829(1)	(1)–(2)	2.848(1)	(4)–(5)	2.834(1)
(1)–(3)	2.867(1)	(1)–(3)	2.846(1)	(4)–(6)	2.872(1)
(2)–(3)	2.783(1)	(2)–(3)	2.815(1)	(5)–(6)	2.787(1)
Allyl group (Å)					
3a		**3b**(A)		**3b**(B)	
Ru(2)–C(74)	2.203(8)	Os(2)–C(74)	2.234(21)	Os(4)–C(84)	2.230(17)
Ru(2)–C(75)	2.234(9)	Os(2)–C(75)	2.244(21)	Os(4)–C(85)	2.263(17)
Ru(2)–C(76)	2.369(10)	Os(2)–C(76)	2.303(18)	Os(4)–C(86)	2.290(18)
C(74)–C(75)–C(76): 125.7(9)°		C(74)–C(75)–C(76): 120.1(1.8)°		C(84)–C(85)–C(86): 121.6(2.0)°	
Semi-bridging CO (Å)					
3a		**3b**(A)		**3b**(B)	
C(22)–Ru(2)	1.939(9)	C(22)–Os(2)	1.918(20)	C(52)–Os(5)	1.896(21)
C(22)–Ru(3)	2.396(9)	C(22)–Os(3)	2.614(19)	C(52)–Os(6)	2.570(20)
Ru(2)–C(22)–O(22): 153.2(8)°		Os(2)–C(22)–C(22): 161.3(1.8)°		Os(5)–C(52)–O(52): 160.3(1.9)°	

[a] Atoms are labelled as given in Figs. 1 and 2. E.s.d. of the last one or two digits cited is given in parentheses.

*Formation and placement of the η^3-methallyl group in **3a** and **3b**.* We find significant the formation of an η^3-methallyl group bonded to a single metal center, by contrast to its more prevalent coordination to three metal centers as in $Ru_3\{\mu\text{-}H,\eta^3,\mu\text{-}EtC{=}CH{=}CMe\}(CO)_9$ [9].

Table 5

Selected data for $Ru_2\{\mu\text{-}O{=}C\text{-}CMe{=}CMe(\eta_2\text{-}CMe{=}CHMe\}\{\mu\text{-}O{=}CNMe_2\}(CO)_5$ (**5a**) [a]

Interatomic separations (Å)			
Ru(1)–Ru(2)	2.681(1)	Ru(2)–C(21)	1.970(6)
Ru(1)–C(31)	2.101(5)	Ru(2)–C(22)	1.857(6)
Ru(1)–O(41)	2.154(3)	Ru(2)–O(31)	2.140(3)
Ru(1)–C(11)	1.865(6)	Ru(2)–C(44)	2.393(5)
Ru(1)–C(12)	1.966(6)	Ru(2)–C(45)	2.321(5)
Ru(1)–C(13)	1.940(6)		
		C(41)–C(42)	1.458(7)
C(31)–O(31)	1.281(6)	C(42)–C(43)	1.359(7)
C(41)–O(41)	1.249(6)	C(43)–C(44)	1.511(7)
		C(44)–C(45)	1.366(7)
Angles (°)			
C(11)–Ru(1)–O(41)	165.1(2)	C(21)–Ru(2)–C(41)	169.6(2)
C(12)–Ru(1)–C(31)	164.9(2)	C(22)–Ru(2)–O(31)	167.1(2)
C(13)–Ru(1)–Ru(2)	162.4(2)	C(44)–Ru(2)–Ru(1)	145.0(1)
		C(45)–Ru(2)–Ru(1)	146.7(1)

[a] Atoms are labeled according to Fig. 3. Numbers in parentheses are the estimated standard deviations in the last significant digits.

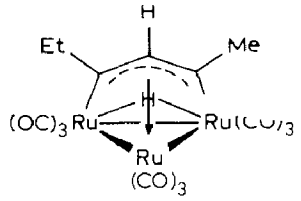

$Ru_3\{\mu\text{-H}, \eta^3, \mu\text{-EtC}{=}{=}\text{CH}{=}{=}\text{CMe}\}(CO)_9$

We propose that the first step in the overall transformation is the initial substitution of the acetylene on the metal atom to which the oxygen of the $\{\mu\text{-O=CNMe}_2\}$ group is bonded. This has been the general substitution pattern observed for all previous studies on the edge double-bridged starting complexes, both with ^{13}CO substitution as well as substitution by phosphines or phosphites [10,11].

Migration of the bridging hydride to such a coordinated acetylene would convert it to the vinyl group $CCH_3{=}CH(CH_3)$ at the same metal center. Finally, hydrogen migration from the α-methyl to the α-carbon atom in the vinyl group would lead to the methallyl complex observed. Precedent for such a migration is provided by the elegant studies of Green, Orpen and co-workers [12] in which the vinyl derivative $CpMo(L)_2(\eta^2\text{-}C(CH_3){=}CPh_2)$, formed by alkylation of the cationic acetylene complex $[CpMo(L)_2(CH_3C{\equiv}CPh)]^+$, is observed slowly to transform (in toluene at 25 °C over 3 days) to the methallyl complex $CpMo(L)_2(\eta^3\text{-}CH_2\text{–}CH\text{–}CPh_2)$. In our studies, no intermediate η^2-vinyl complex could be observed, certainly not in the tri-osmium system which had to be heated to 140 °C, nor in the tri-ruthenium complex which was formed at 23 °C. The methallyl complex **3a** is one of several products observed in the ruthenium system, by contrast to the analog **3b** which is the only product observed in the tri-osmium system (see Scheme 1, above).

Semi-bridging CO in 3a or 3b. A distinctly asymmetric CO bridge [13] is observed between Ru(2) and Ru(3) in **3a**, or between the analogous pairs of atoms in **3b**, namely, Os(1)–Os(2), molecule A, or Os(5)–Os(6), molecule B, see Figs. 1 and 2. The asymmetry in M–C separations is accompanied by a significant bend in the M–C–O angle, see Table 4. In the following analysis, the discussion of the electronic environment in Ru(2) and Ru(3) also pertains to the analogous pairs of Os atoms in **3b**. If for a moment we neglect the metal–metal bond between the two indicated metal atoms, we find an electron count of 18 at Ru(2). By contrast, an electron count of 16 is observed at Ru(3). This may however be increased to 18 through the donation of an electron pair from Ru(2). Thus the metal–metal bond between Ru(2) and Ru(3) (or between the analogous Os atoms in **3b**) must have considerable polarity, a condition that Cotton has identified as leading to the semi-bridging CO [13].

Implication of the oligomerization sequence in 5a. In this product we see a vicinal arrangement of the newly formed μ-acyl group with respect to the $\{\mu\text{-O=CNMe}_2\}$ group of the starting material. The implications of the formation of the dinuclear complex has been discussed above. The formation of the vicinal derivative suggests that the oligomerization sequence was started by coordination of an acetylene to the ruthenium atom to which the oxygen of the $\{\mu\text{-O=CNMe}_2\}$ group was originally attached. This again follows the general substitution pattern mentioned above for the edge double-bridged starting complexes [10,11].

The oligomerization sequence of two acetylenes is *cis,cis*-, culminating with a migration of the metal-bonded part of this chain to a carbonyl group. This contrasts observations in the polynuclear anionic iron complex $[Fe_2(CO)_2\{\mu\text{-}C(C(O)OCH_3)\text{-}C(C(O)OCH_3)C(O)C(C_6H_5)H]^-$ [14], where a *trans*-vinyl group is separated from a *cis*-vinyl group by an inserted CO. Although we draw attention to structural comparisons between **5a** and the binuclear iron complex, no inferences

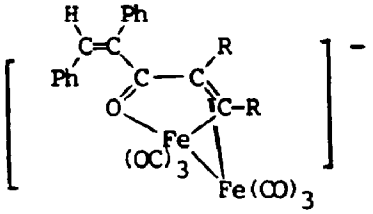

$[Fe_2(CO)_2\{\mu\text{-}C(C(O)OCH_3)C(C(O)OCH_3)C(O)C(C_6H_5)C(C_6H_5)H]$

are implied for differences in reactivity due to differences in the metal atoms because of many other differences in the two reaction systems.

Conclusion. The enhanced reactivity of the edge double-bridged starting materials has permitted us in the case of ruthenium to observe some interesting transformations at rather mild temperature as compared to conditions required to bring the parent $Ru_3(CO)_{12}$ into reaction. Unique products are obtained in both the tri-ruthenium as well as the tri-osmium systems, the latter requiring somewhat more elevated temperatures to be brought into reaction.

The position of the allyl group in products **3a** or **3b** as well as the point of attachment of the μ-O=C–CMe=CMe(η^2-CMe=C(H)Me group suggest that initial substitution of acetylene occurs on the metal to which the oxygen of the μ-O=CNMe$_2$ group is attached, following the path of PR_3 or ^{13}CO substitution observed for these and related edge double-bridged derivatives.

Acknowledgment

This work was supported by the National Science Foundation (Grant CHE-84-05517), a NATO fellowship from the DAAD (German Academic Exchange Service) to W.J. Sieber, and a NATO-SERC fellowship to N.M. Boag.

References

1 C.E. Kampe, N.M. Boag and H.D. Kaesz, J. Mol. Catal., 21 (1983) 279.
2 (a) C.M. Jensen, Y.-J. Chen and H.D. Kaesz, J. Am. Chem. Soc., 106 (1984) 4046; (b) C.M. Jensen, Y.-J. Chen, C.B. Knobler and H.D. Kaesz, New. J. Chem., 1 (1988) ●.
3 (a) A. Mayr, Y.-C. Lin, N.M. Boag and H.D. Kaesz, Inorg. Chem., 21 (1982) 1704; (b) R. Szostak, C.E. Strouse and H.D. Kaesz, J. Organomet. Chem., 191 (1980) 243.
4 Y.-C. Lin, A. Mayr, C.M. Knobler and H.D. Kaesz, J. Organomet. Chem., 272 (1984) 207.
5 (a) W. Krone-Schmidt, W.J. Sieber, N.M. Boag and C.B. Knobler and H.D. Kaesz, Abstr. Papers 190th National Am. Chem. Soc. Meeting, Chicago, IL, 8–13 Sept. 1985, Paper No. INOR 26; (b) idem. Tracing the Pathways of Reactive Intermediates on Metal Cluster Complexes, Homogeneous and heterogeneous catalysis, Proc. Fifth Intern. Symp. Relations Between Homogeneous and Heterogeneous Catalysis, Novosibirsk, 15–19 July 1986, Yu. Yermakov and V. Likholobov (Eds.), VNU Science Press, Utrecht, Netherlands, 1986.
6 W. Krone-Schmidt, W.J. Sieber, C.B. Knobler and H.D. Kaesz, manuscript in preparation.

7 (a) International Tables for X-Ray Crystallography, Vol. IV, Kynoch Press, Birmingham, 1975; (b) R.F. Stewart, E.R. Davidson and W.T. Simpson, J. Chem. Phys., 42 (1965) 3175.
8 M.R. Churchill, F.J. Hollander and J.P. Hutchinson, Inorg. Chem., 16 (1977) 2655.
9 (a) M. Evans, M. Hursthouse, E.W. Randall, E. Rosenberg, L. Milone and M. Valle, J. Chem. Soc., Chem. Commun. (1972) 545; (b) G. Gervasio, D. Osella and M. Valle, Inorg. Chem., 15 (1976) 1221; (c) cf. E. Sappa, A. Tiripicchio and P. Braunstein, Chem. Revs., 83 (1983) 203–239.
10 A. Mayr, Y.-C. Lin, N.M. Boag, C.E. Kampe, C.B. Knobler and H.D. Kaesz, Inorg. Chem., 23 (1984) 4640.
11 C.E. Kampe and H.D. Kaesz, Inorg. Chem., 23 (1984) 4646.
12 S.R. Allen, R.G. Beevor, M. Green, N.C. Norman, A.G. Orpen and Ian D. Williams, J. Chem. Soc. Dalton Trans., (1985) 435.
13 (a) F.A. Cotton, Prog. Inorg. Chem., 21 (1976) 1; (b) F.A. Cotton, L. Kruczynski and B.A. Frenz, J. Organomet. Chem., 160 (1978) 93.
14 J. Ros, X. Solans, M. Font-Altaba and R. Mathieu, Organometallics, 3 (1984) 1014.